Heliyon 8 (2022) e10130

Contents lists available at ScienceDirect

Heliyon

journal homepage: www.cell.com/heliyon

Research article

Preparation of green film with improved physicochemical properties and enhanced antimicrobial activity using ingredients from cassava peel, bamboo leaf and rosemary leaf

Teklu Gadisa Tafa [a], Adam Mekonnen Engida [a,b,*]

[a] Department of Industrial Chemistry, Addis Ababa Science and Technology University, Addis Ababa, Ethiopia
[b] Nanotechnology Center of Excellence, Addis Ababa Science and Technology University, Addis Ababa, Ethiopia

ARTICLE INFO

Keywords:
Biodegradable film
Hydrophilic
Cassava peel starch
Antimicrobial activity
Essential oil
Silica nanoparticle

ABSTRACT

Persistent petroleum based plastic polymers are posing a threat to the environment and human health. Hence, preparation of eco-friendly packaging materials from natural sources is innovative idea to replace persistent plastic films. However, biodegradable films from biomass absorb water that can promote bacterial growth and affect lifetime of film as well as the packed products. In this work, new biodegradable film with improved antimicrobial activity, physicochemical property and less water absorbing and holding property is prepared from modified blend of cassava peel starch (CPS), silica nanoparticle (SNP), glycerol plus rosemary essential oil (REO). The mixture (blend) of CPS, SNPs and glycerol in measured amount of distilled water was treated with acetic anhydride to reduce hydrophilic nature of the blend before adding REO. The content of SNPs in the biofilm was optimized by varying the concentration of SNPs (0.2–0.8%; w/w) keeping other factors constant. Based on the characterization results, the physicochemical property of the biofilms was dependent on the content of SNPs and the best result (film) has been found with 0.6% SNPs which was considered as optimum amount for further experiments. The film prepared from modified blend with 0.6% SNP had shown low water absorption, low water vapor transition rate, improved thermal stability, and less biodegradability. Based on the image from profilometer, the modified blend had shown better homogeneity with REO than unmodified blend and the film with REO had shown better antimicrobial activity as compared to the film without REO (control). The antimicrobial activity of the film with REO was also compared with reference (gentamicin) and its activity was comparable and promising. In general, the prepared film had shown improved physicochemical properties and enhanced antimicrobial activity.

1. Introduction

Due to the plastics' chemical and mechanical properties and particularly due to their persistency, plastic polymers are posing a threat to the environment (Harmaen et al., 2015). To reduce this environmental impact and support environmental sustainability new materials and innovative methods are required (Elleuch et al., 2018). Environmental friendly and natural based plastic materials have acquired great consideration due to increasing health concerns and environmental problems caused by conventional plastics, due their persistence in the environment and leakage of its toxic additives (Wu et al., 2019). Development of eco-friendly bio-based packaging materials from natural polymers such as proteins, cellulose, poly lactic acid (PLA), starch, chitosan, agar is an innovative idea (Perumal et al., 2018). Natural polymers from agro-wastes are promising resources to substitute petroleum based plastics due their natural availability, biocompatibility, low price, non-carcinogenic, non-toxic and ability to form films (Reshmy et al., 2021). Current ongoing research aims to meet the environmental legislation and consumer demands for innovative and sustainable food packaging (Merino et al., 2019).

Even if starch has promising characteristics for film preparation, it has drawbacks: hydrophilic nature, brittleness, low thermal stability, high susceptibility to microorganism, high moisture absorption and poor mechanical properties that limit its applications in packaging industries (Yuan et al., 2021). The high moisture absorption property of biofilms promotes microbial growth and reduces the lifetime of films and the shelf

* Corresponding author.
E-mail address: adam.mekonnen@aastu.edu.et (A.M. Engida).

https://doi.org/10.1016/j.heliyon.2022.e10130
Received 19 April 2022; Received in revised form 2 June 2022; Accepted 28 July 2022

life of packed products which is the biggest challenge of packaging industry. There are previous reported films prepared from starch treated with acetic anhydride to reduce the hydrophilic nature of films (Farajpour et al,. 2020).

However, the literature review does not show and explain the poor compatibility of modified starch with SNP and glycerol having hydrophilic nature. The modified starch is expected to be less hydrophilic; as a result its chemical interaction with polar glycerol and SNP will be reduced and lead to poor physicochemical properties and expected to hold high moisture content. This is a limiting factor for the short service life and poor performance of films prepared from biomass. Again the whole content (SNP, glycerol and modified starch) is not chemically compatible with essential oil.

Hence, the first objective of this study was to prepare film from biomass with improved physicochemical properties by considering chemical compatibility of the whole constituting ingredients. Polar ingredients: CPS (matrix), glycerol (plasticizer) and SNP (filler) (which are chemically compatible) were mixed in a measured amount of distilled water and the whole content was considered as a blend. During mixing, the expected reactions are: glycerol forms new hydrogen bond with starch by destroying the existing hydrogen bonds between starch chains and loosen interaction between chains as result it increases elasticity of the matrix. SNP has both physical and chemical interaction with the matrix (starch). Physically, SNP fill the pores/openings in the starch structure, hence reduces water holding capacity of the film (Alizadeh-Sani et al., 2018). Additionally, SNPs forms hydrogen bonds with remaining OH groups in the blend and O–Si–O of SNP. The second objective of this research is to enhance antimicrobial activity of the film by homogenizing REO with the whole content (blend). To achieve these objectives, the blend of CPS, SNP and glycerol was modified as a whole by treating with acetic anhydride to enhance hydrophobicity and to reduce water absorbing property of the final film. In addition to this, hydrophobicity of the blend helps to increase mixing of the blend with REO which is added to enhance the antimicrobial activity of the final film product. The optimum quantity of SNP in the blend was determined by varying its concentration, keeping other factors constant. The prepared films were studied using selected analytical techniques; Fourier transform infrared (FTIR), Tensile tester and Optical surface profilometer (OP). Based on physicochemical and antimicrobial activity of the films, the new film had shown good thermal stability; less moisture absorption property, good tensile strength as compared to previous report and it has also shown excellent antimicrobial activity in reference to experimental control and gentamicin.

2. Materials and method

2.1. Chemicals, apparatus and instruments

To accomplish this study, the following chemicals and instruments were used. Namely: sodium hydroxide (98%, analytical reagent, India), sulfuric acid (98%, analytical reagent, India), glycerol ($C_3H_8O_3$) (>99.7% Malaysia), Methyl red (96%, analytical reagent, India), hexane (Reagent >99.8%), boric acid (99.9%, Guangzhou Tengyue chemicals co., Ltd.), Acetic anhydride (99%, Northampton, Uk), Ethanol (99%, Absolute HPLC grade, Spain), hydrochloric acid (37%, Analytical reagent), anhydrous sodium sulphate (Na_2SO_4) (99.0%, Research-lab fine chem industries, India), Mueller Hinton Agar (MHA) (HIMedia Laboratories Pvt Ltd., India), Borax ($Na_2B_4O_7.10H_2O$) (99%, Abron Chemicals, India), soxhlet extraction unit (Buchi E-E 816), onion chopper (Rani HHC-885, Germany), pH meter (Hanna, H 5521, Romania), analytical balance (AUW320), oven (Fisher scientific, 40GCEMD), hot plate (AM 5250A), muffle furnace (Britain R00010000), heating mantle (Temperature Controller 500Ml), zetasizer nano series (MAL 1149420), Tensile strength tester (Tensile tester (XLW)), Protein Analyzer (Auto kjeldahl) (Switzerland,K-370), Digital ultra-sonication bath (Labman Scientific, LMUC-2.8L, India), centrifuge (MPW-350R, Poland), Fourier transform infrared spectrometer (FTIR) (iS50, Germany), Differential scanning calorimeter (SKZ1052B) and scanning electron microscope (SEM, InspectF50, FEI).

2.2. Methods

2.2.1. Collection of raw materials

Bamboo leaf was collected from west wollega zone, Oromia regional state, Ethiopia and the rice husk was collected from Amhara regional state N. Gonder zone and the Cassava root was from Amaro zone, South nation nationality regional state, Ethiopia.

2.2.2. Pretreatment of cassava peels and starch extraction

The cassava root was washed with tap water and the peel was removed from the root and sun dried before being powdered by onion chopper to facilitate starch extraction. The starch was extracted from cassava peel as shown in Figure 1 based on previously reported method (Arikan and Bilgen, 2019) as follows: 600 g of grounded sample was mixed with 400 mL distilled water in small bucket to form solution and the solution was stirred frequently for 30 min. Then, the solution was filtered using 20 μm sieve into a beaker. The filtrate was allowed to stand for 2 h until the entire starch being settled down and then the supernatant was decanted. The extracted starch was rinsed with distilled water and dried in an oven at 50 °C for 24 h. The dried starch was crushed for further drying at a temperature of 30 °C in an oven for 2 days. Finally, the dried starch was stored in polyethylene bag for film preparation. The percent yield of the extracted starch was determined using Eq. (1) as follows:

$$Starch\ yield\ (\%) = \frac{weight\ of\ extracted\ starch}{weight\ of\ cassava\ peel} \times 100 \quad (1)$$

2.2.3. Proximate analysis of CPS

Composition of the starch: moisture content, crude protein, fiber, ash content and other constituents were determined using respected standard methods. The composition of CPS can be influenced by mineral content in the soil (Hasmadi et al., 2020). The contents of main constituents of the CPS (moisture, fat, ash, fiber, protein and carbohydrate) were determined using AOAC international (2000), method with slight modification.

2.2.3.1. Determination of moisture content. The moisture content of CPS was determined from weight loss of samples using Eq. (2) as follows: five gram of CPS was taken in a pre- Weighed dry dish and placed in a hot air oven at 90 °C and for 3 h until a constant weight was gained. The test was repeated three times and the average percentage of weight loss was considered as moisture content (MC).

$$MC\ (\%) = \frac{m_2 - m_3}{m_2 - m_1} \times 100 \quad (2)$$

where, m_1 – weight of crucible, m_2 – weight of crucible with sample before drying and m_3 – weight of crucible with sample after drying.

2.2.3.2. Determination of crude fat. The crude fat was determined using soxhlet extraction method as described in AOAC international (2000), method (934.01) with slight modification as follows: about 40 g of CPS was weighed accurately and transferred into labeled thimble and 100 mL of hexane was taken in extraction flask and allowed to reflux for 3 h. After refluxing, the solvent was removed using rota evaporator and the remaining residue was taken and allowed to cool in a desiccator. Finally the mass of the extracted (fat) was weighed and the percentage of fat was calculated using Eq. (3) as follows:

Figure 1. Flow diagram for extraction process of CPSs.

$$Fat\ content(\%) = \frac{m_2 - m_1}{m} \times 100 \quad (3)$$

where m_1 is weight of extraction flask, m_2 is weight of extraction flask and sample after drying and m-weight of sample.

2.2.3.3. Determination of ash content. The ash content of CPS was determined by the method described in AOAC (2000), method (900.02). Five gram of CPS was taken in a crucible and overcooked on hot plate. Then it was placed in furnace at 550 °C for 3 h. After combustion, the ash was cooled in a desiccator and its weight was determined. The ash content of the sample was calculated using Eq. (4)

$$Ash\ content(\%) = \frac{w_1 - w_2}{w} \times 100 \quad (4)$$

where, W_1 – weight of crucible with ash, W_2 – weight of crucible and W – Weight of sample taken for analysis.

2.2.3.4. Determination of crude fiber. The crude fiber of CPS was determined based on AOAC international (2000), method (960.52). Three gram (3 g) of dry CPS was taken in 500 mL beaker and 200 mL of 1.25% H_2SO_4 was added. Then, the content of the beaker was boiled for 30 min at 100 °C with constant stirring. After cooling, the solution was filtered using whatman 1 filter paper and the residue was washed with hot water (3×) to neutralize the acid. Then, the residue was transferred into a 500 mL beaker and 200 mL of 1.25% NaOH was added and boiled for 30 min. Then, the content was filtered and the residue was washed with hot water to remove alkalinity before transferring into a pre weighed crucible for drying in an oven at 100 °C for 3 h. The dried residues were overcooked on hot plate until the smoke ceased to come out from the sample and then it was cooled in a desiccator before weighing. The percentage of the crude fiber was calculated by using Eq. (5)

$$Crude\ fiber\ (\%) = \frac{w_2 - w_3}{w_1} \times 100 \quad (5)$$

W_1 is sample weight (g), W_2 is crucible weight with dry sample and w_3 is crucible weight with fiber.

2.2.3.5. Determination of crude protein. Protein content was determined using Kjeldahl method as described in AOAC (2000) standard method (991.43) with slight modification. Two (2) g of CPS was placed in a 100 mL digestion flask and 50 mL of concentrated sulphuric acid was added to the sample with vigorous shaking.

Then, the content was heated on mantle in fume hood until clear solution was obtained. The clear solution was cooled to room temperature and 25 mL boric acid (2%) and 2 drops of methyl red were added into the sample. Then 20 mL of 40% NaOH was added to the digested sample and heated for 5 min followed by titration with 0.1 N HCl until it became colorless. Finally, the crude protein content was determined indirectly Eq. (6b) from the calculated nitrogen using Eq. (6a).

$$\%\ Nitrogen = \frac{100(VA - VB) \times NA \times 0.01401 \times 100}{w \times 10} \quad (6a)$$

$$\text{Crude proten content} = \%\ \text{Nx}6.25 \quad (6b)$$

where, VA – Volume of standard acid (mL), VB – volume of base, NA – Normality of HCl, W – Weight of sample and 6.25 is nitrogen to protein conversion factor.

2.2.3.6. Determination of carbohydrate content. The carbohydrate content of the CPS was determined using a method reported by Ojo et al. (2017) and the carbohydrate content was determined from other proximate analysis using Eq. (7).

$$\text{Carbohydrate content (\%)} = 100 - (\%\ \text{protein} + \%\ \text{moisture} + \%\ \text{fat} + \%\ \text{ash}) \quad (7)$$

2.2.4. Extraction 228 of SNPs from rice husk, and bamboo leaf

SNPs were extracted from rice husk and bamboo leaf using a method adapted from previous studies (Patil et al., 2018) (Figure 2). The collected bamboo leaf and rice husk were first washed with tap water and sun dried for 4 days followed by oven drying for 3 h at 100 °C. The dried leaf and rice husk were reduced in size and 560 g of each was taken separately and combusted at 600 °C for 3 h in the Muffle furnace. Then the collected bamboo leaf ash and rice husk ash were taken separately in 500 mL of 2.5 M NaOH aqueous solution and heated at 100 °C for 4 h under vigorous stirring. After cooling to room temperature, the obtained solution was filtered using whatman 1 filter paper and the filtrate was titrated with 10 M H_2SO_4 under vigorous stirring to precipitate silica. After silica was precipitated, the solution was stirred for 8 h to minimize agglomeration and it was left for 24 h for stabilization. The formed gel was washed with distilled water to remove sulfate salt before drying in the oven. Finally, the synthesized SNPs were stored in a desiccator for further experiment.

Expected reaction scheme:

$$2NaOH + \text{Rice husk ash/ Bamboo leaf ash} \rightarrow Na_2SiO_3 + H_2O$$

$$Na_2SiO_3 + H_2SO_4 \rightarrow SiO_2 + Na_2SO_4 + H_2O$$

2.2.5. Average size determination of SNPs

The sizes of SNPs from bamboo leaf and rice husk were analyzed by particle size analyzer to study the average particle diameter (nm) of SNPs. From each source, 1 g of SNPs was suspended in 10 mL ethanol and the solution was stirred at 25 °C for 15 min. The SNPs suspension was filled in cuvette up to ¾th of its volume and placed in dynamic light scattering chamber. The graph of average particle size distribution (diameter, nm) was recorded as size distribution (nm) vs intensity (%).

2.2.6. Surface characterization of the SNPs

The surface morphology of SNPs obtained from bamboo leaf and rice husk was evaluated using SEM. During imaging, the sample was coated with copper to improve conductivity of the surface and to avoid surface

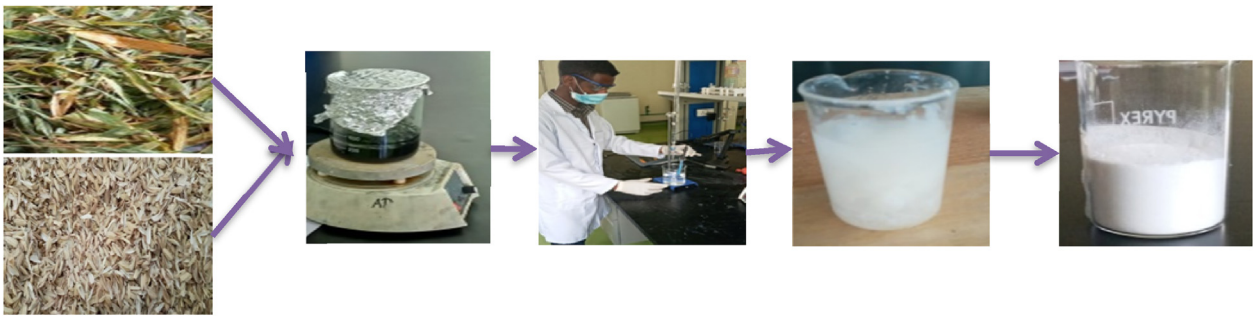

Figure 2. SNPs extraction process.

charge up. Then the images were collected at different magnifications to obtain pictures with optimum resolution.

2.2.7. Extraction of REO

Plant essential oils are reported as antimicrobial agent when they are being used as an ingredient of soap, shampoo and composite film. For similar purpose, essential oil was extracted from rosemary leaf based on previously designed method (Solomon Hailemariam, 2016). About 600 g of wet rosemary leaf was added in to 1 L clean distillation flask and the extraction was done using steam distillation for 3 h. After distillation, the oil was separated carefully and enough anhydrous sodium sulphate was added to the distillate to remove moisture from the REO. The percent yield of the essential oil was determined using Eq. (8).

$$oil\ yield(\%) = \frac{\text{weight of extracted oil}}{\text{weight of rosemary leaves}} \times 100 \quad (8)$$

2.2.8. Film preparation

The film was prepared as follows: 40 g of CPS was suspended in separate 5 beakers (500 mL) with 100 mL of distilled water. Then, SNPs of different concentrations (0.0, 0.2, 0.4, 0.6 and 0.8%: w/w) were slowly added before adding 6% glycerol to each beaker with continuous stirring. The content of glycerol was taken from previous study which was reported as optimum concentration (Alizadeh-Sani et al., 2018; Arezoo et al., 2020). Following that, the solutions were treated with 5 mL of acetic anhydride at pH of 7.5 with stirring for 5 min to modify the chemical nature of the content. Then, the content was heated for 45 min at 85 °C under constant magnetic stirring (2400 rpm) to gelatinize the solutions. After cooling, the gelatinized blend was mixed with 3% REO and stirred slowly for 10 min to homogenize the content. Finally, contents were casted on rectangular shape glass and covered with aluminum foil and left for 2 days in air to dry. Then the dried films were peeled off from the glass and dried in an oven at 50 °C for 3 h. After cooling, they were kept in a polyethylene bag and stored in desiccators for characterization.

2.3. Film characterization

2.3.1. Moisture content (MC)

The MC of the film was determined by weight loss variations before and after drying of the film as of Kan et al. (2019). The biofilms with different content SNPs were cut into 4 cm × 4 cm square pieces and weighed (wi) and kept in an oven at 105 °C with continuous weight determination until it got constant (Wf). The average moisture content was considered from triplicate experiments. The result was calculated using Eq. (9).

$$MC\ (\%) = \frac{w_i - w_f}{w_i} \times 100 \quad (9)$$

where w_i (g) was the initial weight of the samples and w_f (g) was the weight of the samples after oven drying.

2.3.2. Water absorption (WA)

WA of the biofilms was determined based on ASTM D 570, 2004. The films were cut into 4 cm × 4 cm square and specimens were dried in hot air oven at 60 °C until constant weight (wi) was obtained. Then, the dried films were placed in beakers containing distilled water at room temperature and the samples were continuously weighed every day for 1 weak until constant weight (wf) was obtained. Finally, the percentage of absorbed water was calculated for each sample from triplicate experiments using Eq. (10).

$$MA(\%) = \frac{W_f - w_i}{w_i} \times 100 \quad (10)$$

where w_i was the initial weight of the specimen and w_f was the weight of specimen after immersion.

2.3.3. Water vapor transmission rate (WVTR)

The WVTR of the biofilms was determined based on the method designed by Rahim et al. (2020) as follows: the chamber (jar) with a diameter of 10 cm and a height of 12 cm was first adjusted to relative humidity of 75% by adding a solution of 50% NaCl (w/v). Then an acrylic cup with a diameter of 3 cm and height of 1.6 cm was filled with 6 g silica gel, covered with the biofilm of size 6 cm × 8 cm and placed in the moisturized chamber. The mass of the film with the whole set up (film with acrylic cup and silica gel) was weighed before the experiment. The WVTR of the films was determined by weighing the sample every hour for half day. Finally, the WVTR was calculated using Eq. (11).

$$WVTR\ \left(g/h/m^2\right) = \frac{\Delta W}{A} \quad (11)$$

where ΔW is the weight of water transferred to the content through the film per hour (g/h) and A – Surface area of the film (m^2).

2.3.4. FTIR analysis SNP, films and REO

The FTIR spectra of SNP from bamboo leaf, the film from unmodified blend and the film from modified blend without and with REO were obtained to study chemical nature of these items. The analysis of SNPs was performed by conventional potassium bromide (KBr) pellet method as follows: 0.1% of the sample was mixed with 250 mg of KBr powder and homogenized by grinding with pestle and mortar. The ground sample was put into pellet forming die to form pellet size of 13 mm. On the other hand, the films from modified blend (with and without REO) and the film from unmodified blend were analyzed by taking the required size of the films. All samples were scanned in the range of 4000–500 cm^{-1} (Patil et al., 2018).

2.3.5. Mechanical strength of the biofilm

The tensile strength tester was used to study the effect of SNPs on tensile strength and elongation at break values of the film based on ASTM D882-12 standard test method at Sansheng pharmaceutical industry PLC,

Dukam industrial park, Ethiopia. The films were cut into strips with 100 mm length and 13 mm width in dumbbell shape and the samples were conditioned in to the standard atmosphere for testing and the tensile strength and the percentage elongation at break were calculated using Eqs. (12) and (13) respectively.

$$TS\ (MPa) = \frac{F}{A \times T} \tag{12}$$

where F – applied force (N), A – area of film measured (mm^2) and T – thickness of the film (mm).

$$\%\ E = \frac{L_1 - L_o}{L_o} \times 100 \tag{13}$$

where L_1 – Length of tested film at breakage, L_o – Original length of the film.

2.3.6. Biodegradability test

Degradation test helps to study the biodegradability of the bio-based films. The biodegradability of the films was determined based on ASTM 6400 method and ASTM D 5988-12, 2014. The biodegradability test was done by burring specimens (films from unmodified and modified blend) in a soil at 10 cm depth for varied burial duration (15, 30, 45, 60, and 90 days). The loss of masses of the samples was considered to determine biodegradability of the samples. The buried samples were washed with water followed by oven drying at 80 °C for 2 h prior to weighing. The loss of mass of the samples was calculated using Eq. (14).

$$Biodegrability\ (\%) = \frac{w_i - w_f}{w_i} \times 100 \tag{14}$$

where w_i and w_f are initial and final mass of the samples.

2.3.7. Film surface analysis using optical profilometer

The surface morphology of control film (from unmodified) and modified film with 0.6% SNP were imaged using Optical profilometer (Zeta 20 3D profiler) at Addis Ababa Science and Technology University central Laboratory. Similarly, the film from modified blend with 0.8% SNP was analyzed for comparison. The sample was analyzed at magnification of 4000×, with 48 μm sample (pixel) size and 1743 μm × 1308 μm scanned area.

2.3.8. Thermal properties of the films

The thermal properties of the films were determined by Differential scanning calorimetry (DSC) (SKZ1052B) at Addis Ababa Science and Technology University central Laboratory. About 10 mg samples were sealed in aluminum pans and heated from 20 to 300 °C at scan rate of 10 °C/min under argon atmosphere with a flow rate of 25 mL/min using empty aluminum pan as reference and the spectra were recorded to determine the glass transition temperature (Tg) melting (To) and gelatinization temperature.

2.3.9. Evaluation of antibacterial potency of films

The antimicrobial activity of the REO, the prepared films (with and without REO) and the reference (gentamicin) was evaluated against two pathogenic bacteria by disk diffusion method at Addis Ababa Science and Technology University, Biotechnology department. The active cultured bacteria strain (*Escherichia coli and Staphylococcus aureus*) suspension was spread on the Mueller Hinton agar plates with the help of sterile cotton swab uniformly as of Ahmadi et al. (2021). The films with 2 mm diameter were cut by paper hole puncher and placed under UV for 30 min to free from any microorganism and then put on agar plate containing bacteria strain. The REO antibacterial test was done by making a hole on agar medium to reduce the flow of oil. Finally the plates were incubated at 37 °C for 24 h. The anti-bacterial activities of the REO, film samples and the reference were determined by measuring the inhibition zone around hole the containing REO, the sample films, and gentamicin.

3. Results and discussion

3.1. Yield of dry extract from cassava peel

Considerable amount of starch was obtained from dry cassava peel (34.46%). This amount is consistent with previously reported result (35%) which was extracted from fresh cassava by Hauwa et al. (2019). The content of starch obtained from this study is promising to use it as a feed stock for production of films.

3.2. Proximate analysis of CPS

The average moisture content (MC) of CPS was 8.45 ± 0.3% from triplicate experiments. The moisture content in this experiment is lower than previously reported amount (10.43–11.76%) by Chisenga et al. (2019). Higher value of moisture content causes microbial growth as it affects the shelf life of products prepared from starch (Otache et al., 2017). The MC of CPS is in the acceptable range to use it as feedstock for different applications (Chisenga et al., 2019).

The ash content of CPS was found to be 2.13 ± 0.02% and it is in the range of previous reports: 0.7% by Thu (2015) and 4.05% by Otache et al. (2017) from the same source. This variation can be justified because of differences in composition of minerals in soil where the cassava grown (Hasmadi et al., 2020) and also it might be affected by sample treatment and extraction procedures.

In the extract, the protein content was also found to be 2.32 ± 0.01%. This result lays in the range of previous research result (2.07–2.69%) reported from the same material (Hasmadi et al., 2020). The fat content was 0.51 ± 0.01% and it is similar with previous reports: 0.15–0.63 ± 0.05% (Chisenga et al., 2019), 0.74–1.49% and 0.47–1.80% (Thu, 2015). The fiber content in the extract was 2.15 ± 0.03 and it is consistent with previous results (1.10–3.10%) by Thu (2015) and 2.38 ± 0.16 by Hasmadi et al. (2020). The total carbohydrate content in the extract was 84.83 ± 0.10% from dry mass. The carbohydrate content was in the range of previous reports (84.32–86.57%) (Chisenga et al., 2019). Other researchers (Hasmadi et al., 2020) reported lower content of carbohydrates (26.39 ± 0.8–7.02 ± 1.14%) from cassava peel.

3.3. SNPs and their characterization

The yield of SNP extracted from bamboo leaf and rice husk and their size were compared for the purpose of selection. The yield of SNPs from bamboo leaf and rice husk was 21.89% and 23.05% respectively. This result is a little bit lower as compared to previous reports; 28% from rice husk (Sharifnasab and Alamooti, 2017) and 22.63 from bamboo leaf (Irzaman and Irmansyah, 2018). However, other researchers reported relatively lower yield; 18–20% SNPs from rice husk (Setyawan et al., 2019). This variation is expected and might be due to the environmental conditions where the plants grow like other natural products (Ngoc et al., 2018).

The sizes of SNPs obtained from the two samples were determined using Zeta-sizer. The size distribution of SNPs from bamboo leaf and rice husk is shown in Figure 3. The average particle size of the SNP from bamboo leaf (BL) was mainly 7.48 nm (78.6%) (Figure 3a) and the size of SNP from rice husk was mainly about 2759 ± 1273 nm (73.7%) (Figure 3b). Previous researchers reported SNPs with average size of 93.14 nm (Patil et al., 2018) and 60 nm (Sharifnasab and Alamooti, 2017) from rice husk. The size of 78.6% of the SNPs extracted from BL is significantly smaller as compared to the SNPs from RH. The rest 26.4% is above 300 nm which may occur due to aggregation (Lee et al., 2019). In the case of rice husk, most portions of the SNPs were more than 2000 nm. As a result, the SNP from BL was selected as filler in the preparation of the film.

a

Results

			Size (d.nm):	% Intensity:	St Dev (d.n...
Z-Average (d.nm):	3468	Peak 1:	7.481	78.6	0.8569
PdI:	1.000	Peak 2:	319.0	21.4	23.34
Intercept:	0.468	Peak 3:	0.000	0.0	0.000
Result quality :	Refer to quality report				

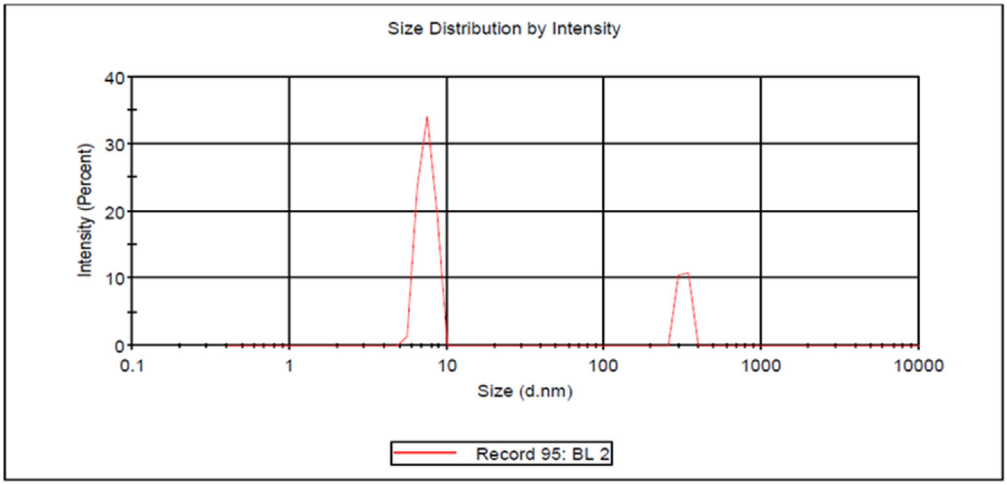

b

Results

			Size (d.nm):	% Intensity:	St Dev (d.n...
Z-Average (d.nm):	129.0	Peak 1:	2759	73.7	1273
PdI:	1.000	Peak 2:	3.129	26.3	0.9960
Intercept:	0.122	Peak 3:	0.000	0.0	0.000
Result quality :	Refer to quality report				

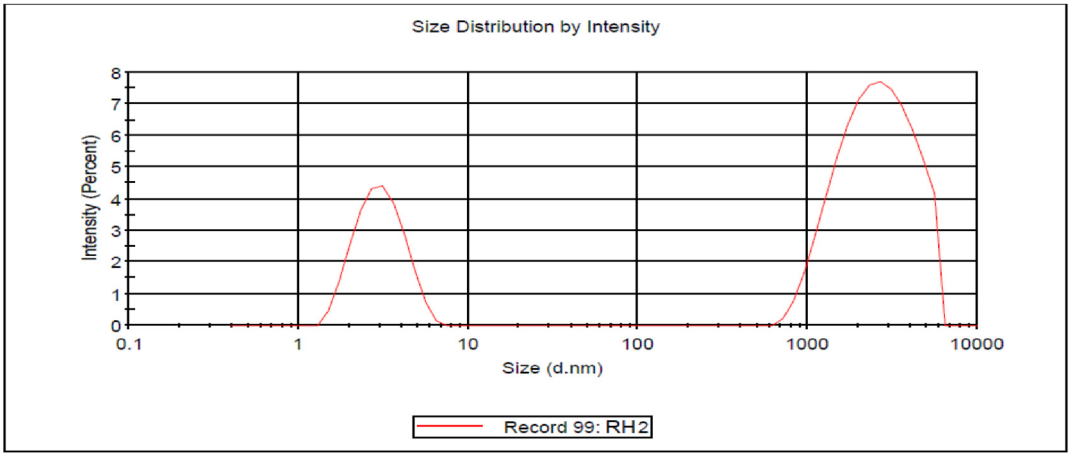

Figure 3. Average particle size distributions of SNPs from a) Bamboo leaf (BL) and b) rice husk (RH).

To determine surface morphology of SNPs, The samples were scanned with magnification of 20,913× as shown in Figure 4 below. It was found difficult to write about the shape of SNPs extracted from both biomasses at given magnification but, the SNPs from BL show little agglomeration (Figure 4a) as compared to RH (Figure 4b). Based on the observed SEM images, there is more agglomeration of particles especially in SNPs obtained from RH (Figure 4b) but, it is difficult to discuss about structure and shape of SNPs at the given condition. Generally, the observed surface features strengthen the information obtained from size analyzer.

3.4. Yield of REO

The yield of REO obtained from Rosemary (*Rosmarinus officinalis*) was 2.87% from wet leave. Anh et al. (2019) reported relatively higher yields of essential oil from wet rosemary leaf (4.818%) which is higher than the current result. This might be due to differences in areas where plants are grown or it might be because of difference in sample handling before and after extraction process. However, the current yield was large enough to use it as additive in this experiment.

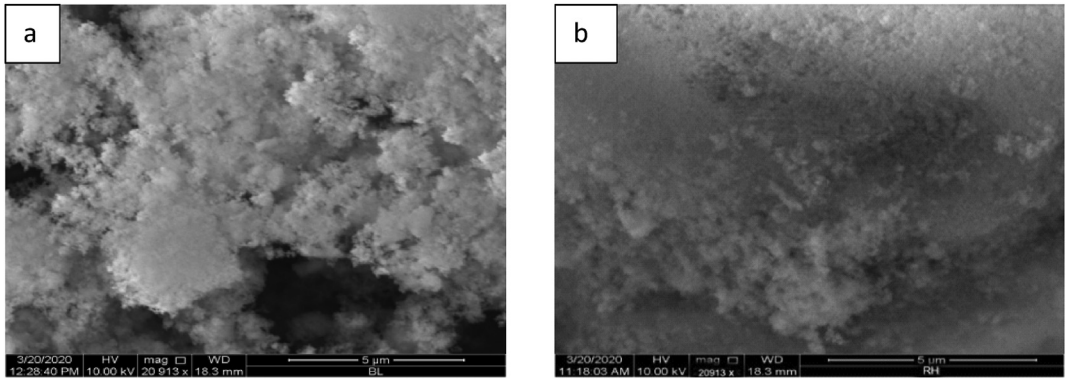

Figure 4. SEM images of SNPs: a) bamboo leaf and b) rice husk.

3.5. Preparation, optimization and evaluation of physicochemical properties of films

The psychochemical properties of the prepared film had shown dependency on the content of SNP. The films prepared from different content of SNPs had shown different MC, WA and WVTR in all cases (Figure 5). The film prepared without filler (0.0% SNP) was considered as control film. The MC (%) of the films was decreased from 24.13 ± 0.01 to 8.92 ± 0.21 as the content of SNPs varies from 0 - 0.6%. The observed MC variation with increasing of SNP might be due to incorporation of SNP in the network structure of starch (Alizadeh-Sani et al., 2018). But, when the concentration of SNPs increased from 0.6 to 0.8%, the MC was increased back to 14.11% which might be due to formation of agglomerates and air spaces as more SNPs are incorporated. Based on the experimental observation, the control film had shown the highest MC (24.13%) as compared to SNP containing films.

The WA value of the film was decreased from 17.32% to 6.03% as the content of SNP varied from 0 to 0.6% (w/w). However, when the amount of SNPs increased to 0.8% the WA of the film was raised to 11.02% as shown in Figure 5. The film with 0.6% SNP had shown low moisture absorption property which might be because of incorporation of SNP into pore spaces available in the matrix.

The study of WVTR is a key parameter for films made from biomass to determine the permeability of vapor through the film. Low WVTR helps to reduce microbial growth and to safeguard the qualities of packed materials (Wang et al., 2021). The control film without filler (0% SNPs) had shown high WVTR (3.08 g/h/m^2). However, WVTR was decreased from 3.08 ± 0.00 to 1.06 ± 0.01 as the content of SNPs increased from 0 to 0.6%. However, when the amount of SNPs increased to 0.8%, the WVTR was raised back to 2.41 ± 0.03. This result is consistent with previous results which were reported by Riahi et al. (2021). Finally, 0.6% SNPs was taken as optimum filler based on the observed WVTR, WA and MC of the film.

3.6. FTIR analysis of SNPs, REO and films

The FTIR spectrum of SNP (Figure 6) shows absorption peaks at 462.839, 794.599 and 1081.888 cm^{-1} due to O–Si–O bending, symmetric stretching and asymmetric stretching respectively (Nhung et al., 2017). The weak absorption band around 3386.26 is related to stretching vibration of O–H on surface of SNPs.

FTIR spectra of the film from unmodified blend and modified blend are shown in (Figure 7). The absorption band at 3445.161 cm^{-1} in both films (films from modified and unmodified blend) corresponds to O–H stretching vibration. However, the peak strength in a film prepared from modified blend was reduced due to the condensation reaction of O–H with –COOH of acetic anhydride. The peak at 2929.38 cm^{-1} in both spectra corresponds to C–H. However, the strength of this peak in the spectrum of modified film is stronger than the peak in the spectrum of unmodified film. This is due to the presence CH_3 group originated from acetic anhydride. The absorption band at 1625 cm-1 in unmodified films is due to carbonyl (C=O) group and the band at 1725 cm^{-1} in modified

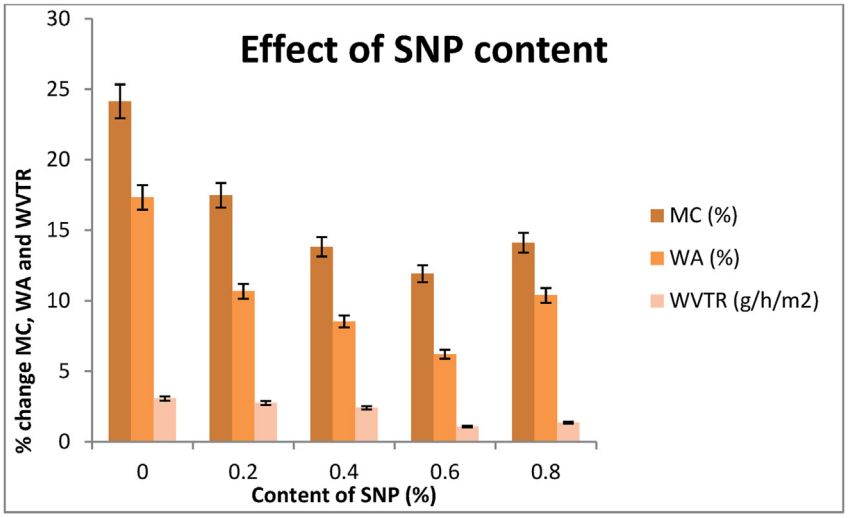

Figure 5. Effect of concentrations SNPs on MC, WA and WVTR% of the biofilm.

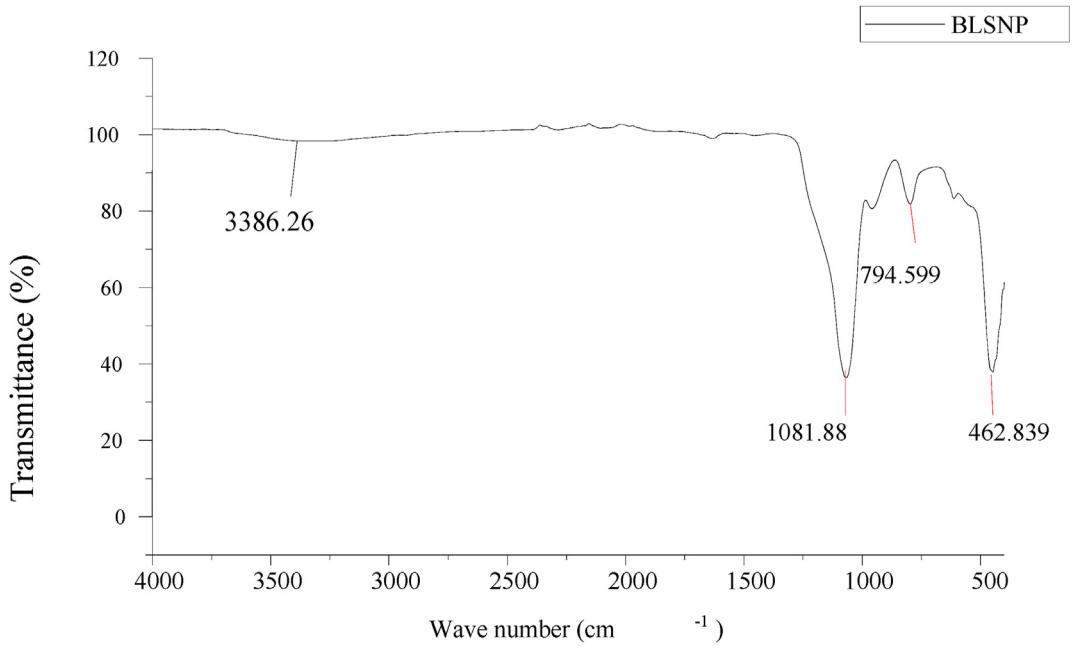

Figure 6. FTIR spectrums of BLSNPs.

film corresponds to carbonyl (C=O) of an ester in the film. The peak at about 998.92 cm^{-1} corresponds to C–O–C stretching of an ester in the modified film (Zhang et al., 2018).

FTIR spectra of the REO and the films with REO and without REO are shown in Figure 8. The absorption peaks around 3332.446 cm^{-1} and 3288.09 cm-1 in the spectrum of REO and in film with REO (MB + REO) respectively corresponds to H–O. However, the strength of this peak in ME + REO is stronger than in the film without REO (MB) (Figure 8) because absorption is additive and it is sum of H–O originated from REO and the blend. The peak at 1739.506 cm-1 and 1741.434 cm^{-1} on both MB and MB + REO spectrum are assigned to the C=O of an ester in the film from modified blend (Shaari et al., 2021). The peak at 1374.24 cm^{-1} and 1008.92 cm^{-1} 497 corresponds to the asymmetric stretching of C–H (Hosseini et al., 2011) and to O–Si–O originated from SNP (Alizadeh-Sani et al., 2018) respectively. Addition of REO into the film has led to the enhancement of peak intensity of the group CH and CH_3 indicating the incorporation of hydrocarbons of REO into the films. The peaks in REO and in the films are similar because of the presence of similar functional groups.

3.7. Mechanical properties of the film

The mechanical property of the films with different content of SNP was evaluated for its tensile strength (TS) (Figure 9a) and elongation at break (Figure 9b). The tensile strengths of the films were 22.472, 25.68, 28.052, 45.64 and 40.86 Mpa for 0.0, 0.2, 0.4, 0.6 and 0.8% SNPs respectively. The control film (0% SNP) exhibited a lower tensile strength (22.472 MPa) while the film with 0.6% SNP had demonstrated a higher value (45.64 Mpa). However, the tensile strength was decreased back to 40.86 Mpa as the content of SNP increased to 0.8%. The incorporation of SNP considerably has affected the tensile strength of the films which is consistent with Zhang et al. (2018) report. At lower concentration of SNP, it would decrease pores and increase bonding between the matrix polymers and improve the adhesion strength in the matrix. However, as concentration of SNPs increased above optimum value (0.6%), it may cause for formation of more space in the matrix because of formation of agglomerate and destroy the integrity of the films (Yadav et al., 2019).

The elongation at break was also increased from 5.2% to 13.8 as the concentration of the SNP raised from 0%, to 0.6%. However, when the

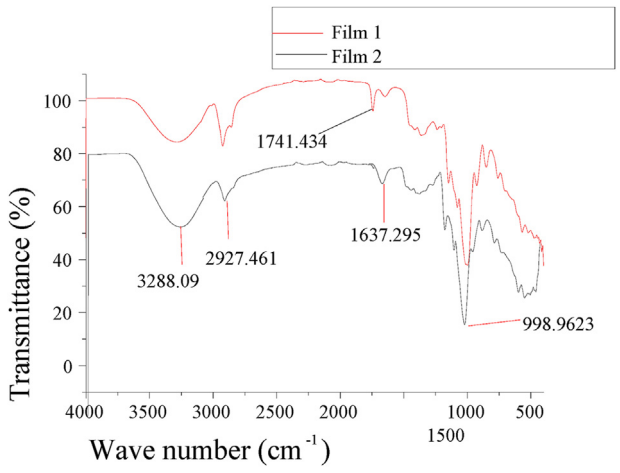

Figure 7. FT-IR spectra of the biofilm from modified blend (Film 1) and un-modified film (Film 2).

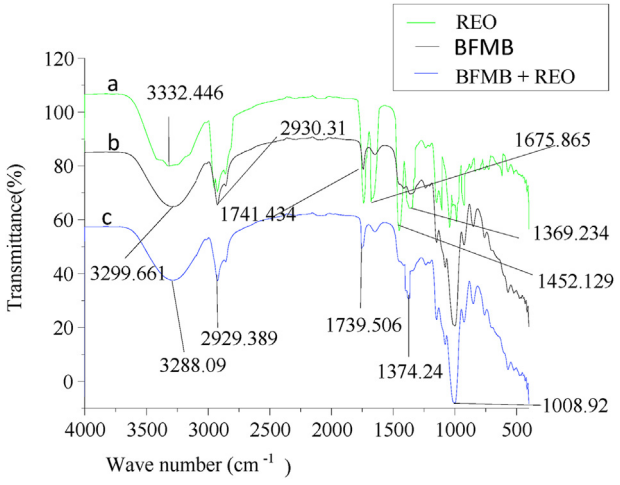

Figure 8. FT-IR spectra of a) REO, b) biofilm from modified blend (BFMB) and c) biofilm from modified blend Plus REO (BFMB + REO).

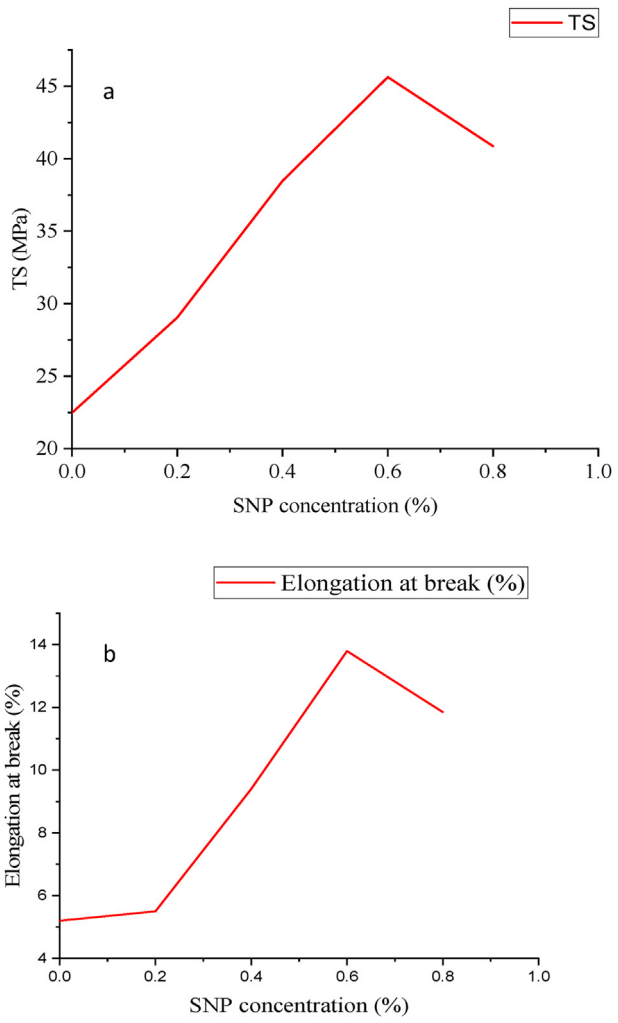

Figure 9. Effect of SNPs concentration on a) Tensile strength (TS) and b) elongation at break of the biofilm.

concentration of SNP increased to 0.8%, the elongation was decreased back to 11.85 (Figure 9b). This indicates a decrease in elasticity of the films when the content of SNPs was increased above 0.6% SNP. The loss in plasticity of the film can be justified by possible poor distribution of fillers in the matrix. The control film had.

3.8. Thermal properties of the film

The thermal behavior of the films prepared from unmodified blend with 0.6% SNP, modified blend with 0.6% and with 0.8% SNP was evaluated using DSC. As it is shown in the DSC curve (Figure 10), the glass transition temperature (Tg) of all the films is not clearly observed in the expected area below 100 °C. In this case, the Tg of the films might be in the lower temperature range and the films would exist in the rubber like state at room temperature (Offiong and Ayodel, 2016). The broad exothermic peak around 100 °C for the film from unmodified blend (Figure 10c) is assigned to the crystalline temperature (Tc) due to the existed crystallite structure of starch in the blend even after gelatinized with glycerol, and the same exothermic peak with reduced size was observed for the film prepared from modified blend with 0.8% SNP (Figure 10b). The size reduction might be because of formation of more amorphous starch structure from leaner chains (Mali et al., 2005) after chemical modification and addition of more filler. However, the same peak has not been clearly observed in the optimized film (Figure 10a) that might be because of formation of amorphous structures even from branched chain starch due to well incorporation of fillers in the film. This result exactly reflects the nature of the film in Figure 11 and it is possible to conclude that all the three activities; addition of glycerol, chemical modification and filler content optimization had played a significant role on the properties of the film.

3.9. The effect of SNPs on surface morphology of the biofilm

The control film (from unmodified blend with 0.6%) (Figure 11a), the films from modified blend with 0.6% SNP (Figure 11b) and with 0.8% SNPs (Figure 11c) were studied using profilometer to determine the surface features of the films. The control film has shown irregular surface with air spaces which look like air bubbles inside the film and it can also be due to incompatibility of the blend with REO (Figure 11a). However, the films from modified blend have shown improved surface features (Figures 11b and 11c) as compared to the control film (Figure 11a). Especially, the film with 0.6% (Figure 11b) had relatively smooth surface and better distribution of REO. This might be because of better distribution of the filler and compatibility of the REO with the modified blend (Alizadeh-Sani et al., 2018). However, the film with 0.8% SNP had shown irregular surface features as encircled in Figure 12c which might

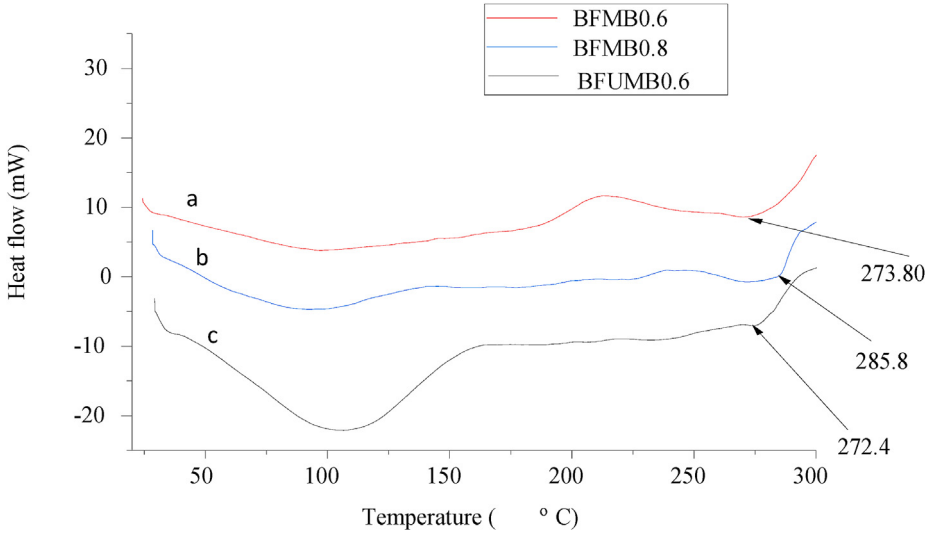

Figure 10. DSC thermograph of a) biofilm from modified blend (0.6%) (BFMB0.6), b) biofilm from modified blend (0.8% SNPs) (BFMB0.8) and c) biofilm from unmodified blend (0.6% SNP) (BFUMB0.6).

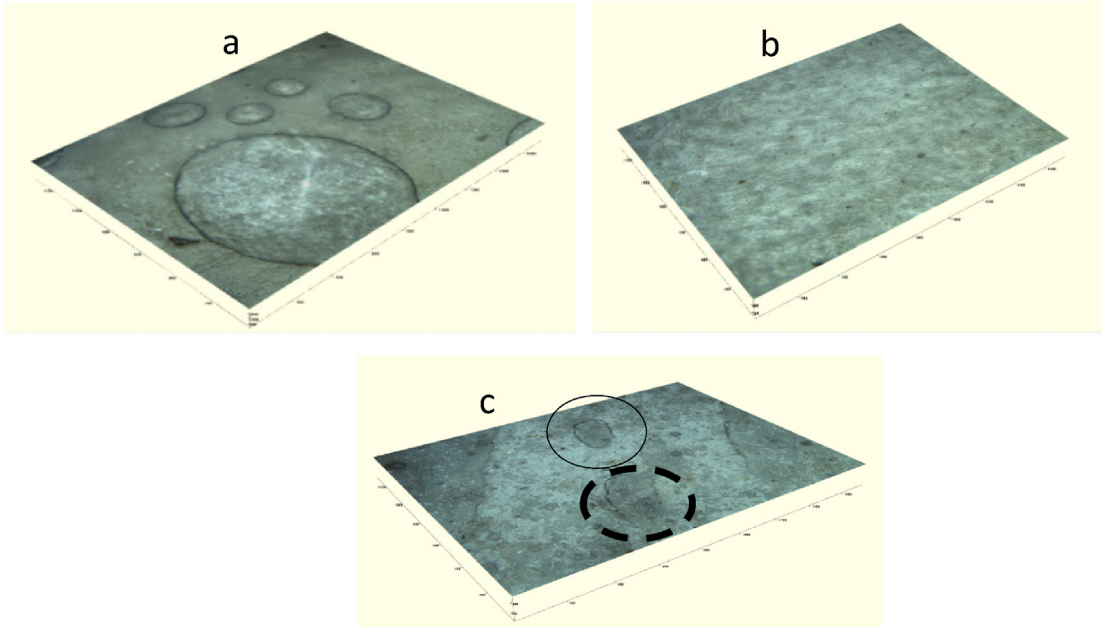

Figure 11. Optical topographic images of (a) the control film, (b) biofilm with 0.6% SNP and c) Biofilm with 0.8% SNP.

be because of induction of agglomeration of SNP in the matrix (Qasim et al., 2020). This uneven distribution of the filler in the prepared film affects its physicochemical properties as well as its efficiency and functionality for the intended purpose. This result clearly shows the importance of blend modification and the effect of SNP content on physicochemical and mechanical properties of the film made from biomass.

3.10. Biodegradability test

Susceptibility for degradation is the critical weakness of film from biomass; as a result biodegradability test is important in this case. The degradability of the films was studied by burying the films in soil having pH around 8.31. Keen follow-up of this experiment had shown various percentage weight losses with burial duration (Figure 12). The purpose of this experiment was to study the effect of chemical modification on degradation of films. In this case both films from modified and unmodified blend contain 0.6% SNP. The percentage weight loss of the control film (from unmodified blend) was 4.69%, 7.71%, 13.28%, and 20.09% within 15, 30, 60 and 90 days respectively (Figure 12a) whereas the percentage degradation of the film from modified blend was 2.15, 5.32, 9.76, 12.66% within 15, 30, 60 and 90 days respectively (Figure 12b). Based on the experimental result, the film from modified blend had shown slow degradation as compared to the control film. The study shows 12.66% loss within 2 months for the film prepared from modified blend and it is low as compared to the weight loss (70%) of the film prepared from unmodified blend (Indumathi et al., 2019). Indumathi et al. reported 70% weight loss for the film prepared from unmodified matrix within 1 month. The current result promotes the contribution of chemical modification to slowdown degradation of films prepared from biomass by reducing moisture absorption because water enhances biodegradation by supporting bacterial growth.

3.11. Antimicrobial activity of the biofilm

Antimicrobial activity of the film (with 0.6% SNP and 0.3% REO) was assessed on selected food poisoning bacteria (*Staphylococcus aureus* (*S. aureus*) and *Escherichia coli* (*E. coli*)) using disc diffusion method. The inhibition potency of the REO, biofilm with 0.6% SNP but without REO and the biofilm with 0.6% SNP and 0.3% REO was compared against

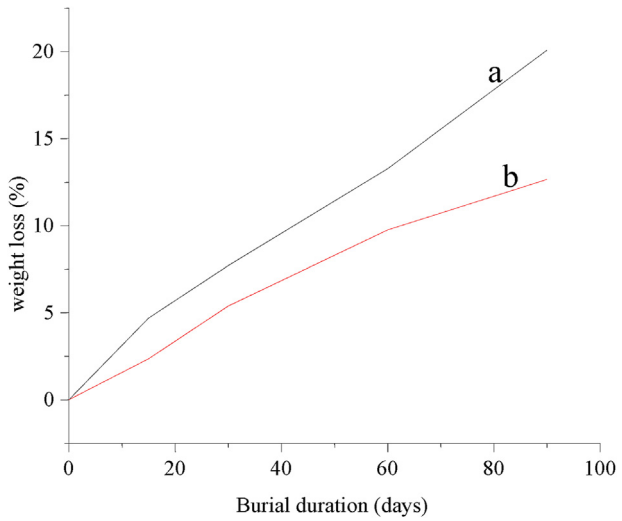

Figure 12. Percentage weight losses of films a) from unmodified blend b) modified blend.

commercial antimicrobial agent (gentamicin) as shown in Figure 13. The REO has shown inhibition activity against tested bacteria with 16.8 and 17.6 mm inhibition zone on *E. coli* and *S. aureus* respectively (Figure 13a). Imamovic et al. (2021) reported almost similar inhibition potential of REO against *E. coli* and *S. aureus* with 17.33 and 18.17 mm inhibition zone respectively. However, REO has shown relatively low inhibition zone as compared to the reference (gentamycin) that has demonstrated strong inhibition activity (Figure 13d). Even if REO has relatively low antimicrobial activity than gentamicin, it has good potency to inhibit bacterial growth.

The film with REO had shown a significant inhibition zone on both *S. aureus* (≈8 mm) and *E. coli* (7.87 mm) (Figure 13c) as compared to the control film (without REO) (Figure 13b) with no clear inhibition zone. The previous report by Amjadi et al. (2020) supports the current result that the film with REO had been reported with good inhibition against both gram negative (*E. coli*) and gram positive (*S. aureus*) bacteria. Hence, incorporation of REO in the film provided a good antimicrobial activity

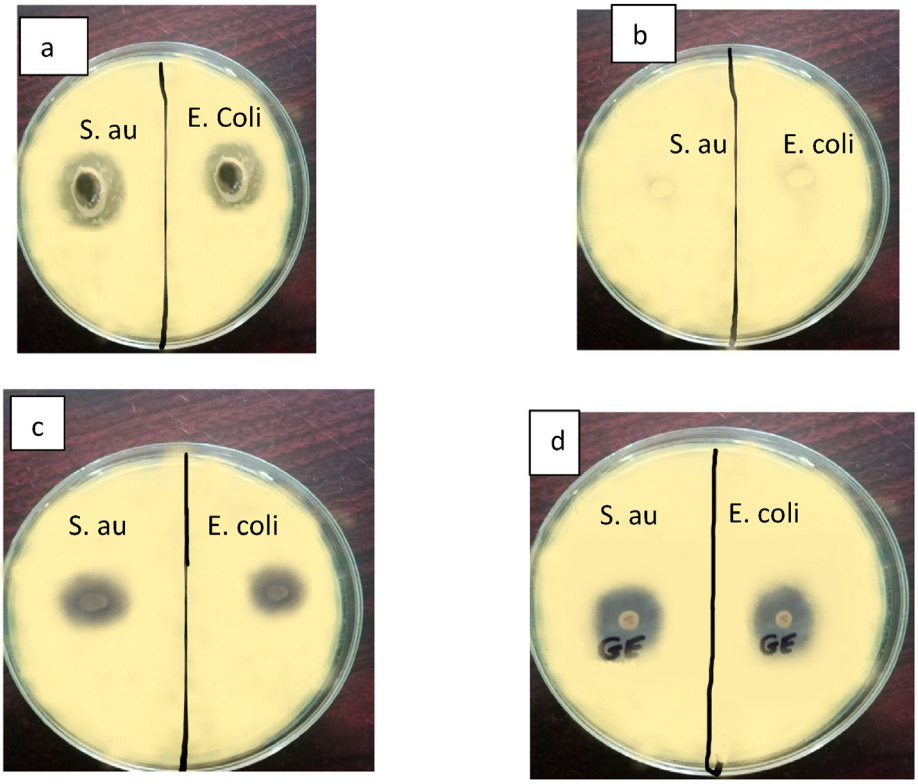

Figure 13. Antibacterial activities of (a) REO (b) control film (with 0.6% SNP but without REO), (c) film with 0.6% SNP and 0.3% REO and (d) Gentamicin against *S. aureus, and E. coli.*

as shown in Figure 13c. This result is promising for production of environmentally friendly films from biomass with good antibacterial activity.

4. Conclusions

The preparation of biodegradable film with improved physicochemical properties and antimicrobial activity was achieved through blend modification as it was confirmed from acquired analytical dada. The ingredients, CPs, SNP and glycerol, are compatible due to their polar nature and the modification of their blend had enhanced the hydrophobic nature of the film. As a result, the prepared film under optimized parameters had shown lower MC, WA and WVTR. Additionally, the compatibility of the blend with REO was increased as it was observed from an image obtained using profilometer and FTIR spectra. The incorporation of REO had shown enhanced antimicrobial property as it was demonstrated on *S. aureus, and E. coli.* The prepared film can be considered as a good competitive advantage in packaging industries with multitude benefits: low cost, less moisture absorbing property, less biodegradable as compared to natural biofilms and good antimicrobial potency. The observed properties of the prepared film and the availability of the resources are promising and make it feasible for mass production with further study.

Declarations

Author contribution statement

Teklu Gadisa Tafa: Performed the experiments.

Adam Mekonnen Engida: Conceived and designed the experiments; Analyzed and interpreted the data; Contributed reagents, materials, analysis tools or data; Wrote the paper.

Funding statement

This research did not receive any specific grant from funding agencies in the public, commercial, or not-for-profit sectors.

Data availability statement

Data will be made available on request.

Declaration of interests statement

The authors declare no conflict of interest.

Additional information

No additional information is available for this paper.

Acknowledgements

We would like to acknowledge Addis Ababa Science and Technology University and Nanotechnology center of excellence at Addis Ababa Science and Technology University.

References

Ahmadi, A., Ahmadi, P., AlizadehSani, M., Ghanbarzade, B., 2021. Functional biocompatible nanocomposite films consisting of selenium and zinc oxide nanoparticles embedded in gelatin/cellulose nanofiber matrices. Int. J. Biol. Macromol. 175, 87–97.

Alizadeh-Sani, M., Arezou, K., Ehsani, A., 2018. Fabrication and characterization of the bionanocomposite film based on whey protein biopolymer loaded with TiO_2 nanoparticles, cellulose nanofibers and rosemary essential oil. Ind. Crop. Prod. 124, 300–315.

Amjadi, S., Almasi, H., Ghorbani, M., Ramazan, S., 2020. Reinforced ZnONPs/rosemary essential oil-incorporated zeinelectrospunnanofibersbyκ-carrageenan. Carbohydr. Polym. 15, 232.

Anh, T.T., Ngan, L.T.T., Lam, T.D., 2019. Essential oil from fresh and dried Rosemary cultivated in Lam Dong province, Vietnam. Mater. Sci. Eng. 544, 012025.

AOAC, 2000. Official Methods of Analysis of AOAC International, seventeenth ed. AOAC International, Md, USA.

Arezoo, E., Mohammadreza, E., Abdorreza, M.N., 2020. The synergistic effects of cinnamon essential oil and nano TiO_2 on antimicrobial and functional properties of sago starch films. Int. J. Biol. Macromol. 157, 743–751.

Arikan, B.E., Bilgen, D.H., 2019. Production of bioplastic from potato peel waste and investigation of its biodegradability. Int. Adv. Res. Eng. 3, 93–97.
ASTM D 570, 2004. Standard Test Method for Water Absorption of Plastics.
ASTM D 5988-12, 2014. Standard Test Method for Determining Aerobic Biodegradation of Plastic Materials in Soil.
ASTM D882, 2015. Tensile Testing of Thin Plastic Sheeting.
Chisenga, S.M., Workneh, T.S., Bultosa, G., Laing, M., 2019. Proximate composition, cyanide contents, and particle size distribution of cassava flour from cassava varieties in Zambia, AIMS Agric. Food 4, 869–891.
Elleuch, B., Bouhamed, F., Elloussaief, M., Jaghbir, M., 2018. Environmental sustainability and pollution prevention. Environ. Sci. Pollut. Res. 25, 18223–18225.
Farajpour, R., Djomeh, Z.E., Moeini, S., Tavakolipour, H., Safayan, S., 2020. Structural and physico mechanical properties of potato starch-olive oil edible films reinforced with zein nanoparticles. Int. J. Biol. Macromol. 149, 941–950.
Harmaen, A.S., Khalina, A., Azowa, I., Hassan, M.A., Tarmian, A., Jawaid, M., 2015. Thermal and biodegradation properties of poly(lactic acid)/fertilizer/oil palm fibers blends biocomposites. Polym. Compos. 36, 576–583.
Hasmadi, M., Harlina, L., Jau-Shya, L., Mansoor, A.H., Jahurul, M.H.A., Zainol, M.K., 2020. Physicochemical and functional properties of cassava flour grown in different locations in Sabah, Malaysia. Food Res. 4, 991–999.
Hauwa, M.M., Dahiru, S., Abdulrahman, B., Abdullahi, I., 2019. Bio-ethanol production from cassava (manihot esculenta) waste peels using acid hydrolysis and fermentation process. Sci. World J. 14, 45–50. www.scienceworldjournal.org.
Hosseini, M.M., Shao, Y., Whalen, J.K., 2011. Bioelements production from silicon-rich plant residues: perspectives and future potential in Canada. Biosyst. Eng. 110, 351–362.
Imamovic, B., Komlen, V., Gavric, T., Sunulahpasic, A., Lalevic, B., Hamidovic, S., 2021. Antimicrobial activity of ginger (*Zingiber officinale*) and rosemary (*Rosmarinus officinalis*) essential oils. AgricultForest 67, 231–238.
Indumathi, M.P., Saral Sarojini, K., Rajarajeswari, G.R., 2019. Antimicrobial and Biodegradable Chitosan/cellulose Acetate phthalate/ZnO Nanocomposite Films with Optimal Oxygen Permeability and Hydrophobicity for Extending the Shelf Life of Black Grape Fruits. Int. J. Biol. Macromol 132, 1112–1120.
Irzaman, O., Irmansyah, N., 2018. Ampel Bamboo Leaves Silicon Dioxide (SiO_2) Extraction. IOP Conf. Ser.: Environ. Earth Sci. Carbohydr. Polym. 224, 1–8.
Kan, J., Liu, J., Yong, H., Liu, Y., Qin, Y., Liu, J., 2019. Development of active packaging based on chitosan-gelatin blend films functionalized with Chinese hawthorn (*Crataegus pinnatifida*) fruit extract. Int. J. Biol. Macromol. 140, 384–392.
Lee, J.,H., Jeong, D., Kanmani, P., 2019. Study on Physical and Mechanical Properties of the Biopolymer/silver Based Active Nanocomposite Films with Antimicrobial Activity.
Mali, S., Grossmann, M.V.E., Maria, A.G., Martino, M.N., Zaritzky, N.E., 2005. Mechanical and thermal properties of yam starch films. Food Hydrocolloids 19, 157–164.
Solomon H/mariam, 2016. Extraction and characterization of essential oil from rosemary leaves. In: A Thesis Submitted to the School of Chemical and Bio-Engineering Presented in Partial Fulfillment of the Requirements of the Degree of Masters of Science in Chemical Engineering (Process Engineering Stream). Addis Ababa University, Ethiopia date: 11/10/2021. https://docplayer.net/59143166-Extraction-and-characterization-of-essential-oil-from796rosemary-leaves.html.
Merino, D., Gutierrez, T.J., Alvarez, V.A., 2019. Structural and thermal properties of Agricultural Mulch films based on native and oxidized corn starch nanocomposites. Starch - Starke., 1800341
Ngoc, N., Thanh, L.X., Vinh, L.T., Anh, B.T., 2018. High-purity amorphous silica from rice husk: preparation and characterization. Vietnam J. Chem. 56, 730–736.
Nhung, D.T., Hoa, T., Trinh, N.T., Phu, D.V., Tuan, P.D., Hien, N.Q., 2017. Synthesis of silica nanoparticles from rice husk ash. Sci. Technol. Dev. J 20, 50–54.
Offiong, E.U., Ayodel, S.L., 2016. Preparation and Characterization of Thermoplastic Starch from Sweet Potato. IJSER. https://www.ijser.org/researchpaper/Preparation-and-Characterization-of-Thermoplastic-Starch-from-Sweet-Potato.pdf. accessed on June 1, 2022.
Ojo, M.O., Ariahu, C.C., Chinma, E.C., 2017. Proximate, functional and pasting properties of cassava starch and mushroom (*pleurotus pulmonarius*) flour blends. Adv. J. Food Sci. Technol. 5, 11–18.
Otache, A.M., Ubwa, T.S., Godwin, A.K., 2017. Proximate Analysis and Mineral composition of peels of three sweet cassava cultivars. Asian J. Chem. Sci. 3, 1–10.
Patil, N.B., Sharanagouda, H., Doddagoudar, S.R., amachandra, C.T.R., Ramappa, K.T., 2018. Biosynthesis and characterization of silica nanoparticles from rice (*Oryza sativa L.*) husk. Int. J. Curr. Microbiol. Appl. Sci. 7, 2298–2306.
Perumal, B.A., Sellamuthu, S.P., Nambiar, B.R., Sadiku, R.E., 2018. Development of polyvinyl alcohol/chitosan bio-nanocomposite films reinforced with cellulose nanocrystals isolated from rice straw. Appl. Surf. Sci. 449, 591–602.
Qasim, U., Ali, M., Ali, T., Iqbal, R., Jamil, F., 2020. Biomass derived fibers as a substitute to synthetic fibers in polymer composites. Chem. Bioeng. 7, 193–215.
Rahim, A., Dombus, S., Kadir, S., Hasanuddin, M., Laude, S., Aditya, J., Karouw, S., 2020. Physical,Physicochemical, mechanical, and sensory properties of bioplastics from phosphate acetylated arenga starches. Pol. J. Food Nutr. Sci. 70, 223–231.
Reshmy, R., Philip, E., Vaisakh, P.H., Shibin, R., Paul, S.A., Madhavan, A., Sindhu, R., Binod, P., Sirohi, R., Pugazhendhi, A., Pandey, A., 2021. Development of an eco-friendly biodegradable plastic from jack fruit peel cellulose with different plasticizers and Boswellia serrata as filler. Sci. Total Environ. 767, 1–8.
Riahi, Z., Priyadarshi, R., Rhim, J., Bagheri, R., 2021. Gelatin-based functional films integrated with grapefruit seed extract and TiO_2 for active food packaging applications. Food Hydrocolloids 112, 106314.
Setyawan, N., Hoerudin, Wulanawati, A., 2019. Simple extraction of silica nanoparticles from rice husk using technical grade solvent: effect of volume and concentration. IOP Conf. Ser.: Earth Environ. Sci. 309, 1–8, 012032, In this issue.
Shaari, S., Samsudin, H., Uthumporn, U., 2021. Effect of acetylation treatment on surface modified tapioca starches. Food Res. 5, 340–347.
Sharifnasab, H., Alamooti, M.Y., 2017. Preparation of silica powder from rice husk. Agric Eng Int :CIGR J. Open 19, 158 access at. http://www.cigrjournal.org.
Thu, S.L., 2015. Modification of Cassava Starch for Biodegradable 797 Plastic Preparation. Department of Industrial Chemistry, Yangon University, pp. 1–93. https://www.academia.edu/16835196/Modification_of_Cassava_Starch_For_Biodegradable_Plastic_Preparation date, 11/10/2021.
Wang, L., Periyasami, G., Aldalbahi, A., Fogliano, A.V., 2021. The antimicrobial activity of silver nanoparticles biocomposite films depends on the silver ions release behavior. Food Chem. 359, 129859.
Wu, C., Sun, J., Lu, Y., Wu, T., Pang, J., Hu, Y., 2019. In situ self-assembly chitosan/ε-polylysine bionanocomposite film with enhanced antimicrobial properties for food packaging. Int. J. Biol. Macromol. 132, 385–392.
Yadav, M., Goswami, P., Paritosh, K., Kumar, M., Pareek, N., Vivekanand, V., 2019. Seafood waste: a source for preparation of commercially employable chitin/chitosan materials. Bioresour. Bioprocess 6, 8.
Yuan, Y., Zhang, X., Pan, Z., Xue, Q., Wu, Y., Li, Y., Li, B., Li, L., 2021. Improving the properties of chitosan films by incorporating shellac nanoparticles. Food Hydrocolloids 110, 106164.
Zhang, Q., Tu, Q., Hickey, M.E., Xiao, J., Gao, B., Tian, C., Heng, P., Jiao, Y., Peng, T., Wang, J., 2018. Preparation and study of the antibacterial ability of graphene oxide-catechol hybrid polylactic acid nanofiber mats. Colloids Surf. B Biointerfaces 172, 496–505.